








Original article

Lower Permian basaltic agglomerate from the Tsengel River valley, Mongolian Altai

Kristýna Hrdličková^{1*} , Altanbaatar Battushig² , Pavel Hanžl¹ ,
Alice Zavřelová¹ , Jitka Míková¹ 

¹ Česká geologická služba, Klárov 3, 118 21 Praha 1, Czech Republic

² Mineral Resources and Petroleum Authority, Barilgachdin talbai-3, Ulaanbaatar 15170, Mongolia

*Corresponding author: kristyna.hrdlickova@geology.cz, ORCID: [0000-0002-7255-9765](https://orcid.org/0000-0002-7255-9765)

ARTICLE INFO

Article history:

Received 4 September, 2020

Accepted 1 November, 2020

ABSTRACT

A new occurrence of Permian volcanic and volcanoclastic rocks in the Mongolian Altai south of the Main Mongolian Lineament was described between soums of Tugrug and Tseel in Gobi-Altai aimag. Studied vitrophyric pyroxene basalt lies in a layer of agglomerate and amygdaloidal lavas, which is a part of NE–SW trending subvertical sequence of varicolored siltstones and volcanoclastic rocks in the Tsengel River valley. This high-Mg basalt is enriched in large ion lithophile elements, Pb and Sr and depleted in Nb and Ta. LA-ICP-MS dating on 44 spots reveals several concordia clusters. The whole rock geochemistry of sample fits volcanic arc characteristic in the geotectonic discrimination diagrams. Dominant zircon data yield Upper Carboniferous and Permian magmatic ages 304.4 ± 2.3 and 288.6 ± 1.9 Ma. Two smaller clusters of Upper Devonian (376 ± 4.7 Ma) to Lower Carboniferous ages (351.9 ± 3.5 Ma) indicate probably contamination of ascending magmatic material. Youngest Triassic age found in three morphologically differing grains reflects probably lead loss. Described high-Mg basalt lava represents sub-aerial volcanism in volcanic arc environment developed over the N dipping subduction zone in the southwestern Mongolia in the time span from Uppermost Carboniferous to Permian during terminal stage of its activity.

Keywords: LA-ICP-MS zircon dating, Permian volcanism, Gobi-Altai zone

INTRODUCTION

The presence and character of volcanic rocks can provide number of valuable geological data enabling to decipher environment and processes of evolution of the particular blocks of the Earth's crust. This scheme can be also applicable for evolution history of the Central Asian Orogenic Belt (CAOB, Mossakovsky et al., 1993), developed between the Siberian

Craton in the north and the Tarim and Sino-Korean blocks in the south, in the time span between 1000 and 250 Ma (Windley et al., 2007).

The continental accretion in the area of the Gobi and Mongolian Altai was accompanied by massive magmatism of volcanic arc character (e.g. Hanžl et al., 2008; Cai et al. 2015; Soejono et al., 2016; Janoušek et al., 2018). Calc-alkaline

subduction-associated magmatism ceased in the region of southwestern Mongolia during the Upper Carboniferous (Hanžl et al., 2020). In this section of CAOB, A-type granitoids and a bimodal alkaline volcanic series developed in the environment analogous to continental rifts during the Permian (Kozlovsky et al., 2015). This contribution describes a new occurrence of Permian volcanic rocks south of the Main Mongolian Lineament in the area of the Tsengel River northwest of the Tseel soum (Gobi-Altai aimag) in the Mongolian Altai. The presented petrological and geochemical data, including radiometric age, complement and specify the lithostratigraphic classification of units in the area which is generally based on the geological map 1: 200,000, sheet L-46-XXIV (Togtokh et al., 1995).

GEOLOGICAL SETTING

The studied locality lies south of a several-kilometers-wide tectonic zone (the Main Mongolian Lineament) separating different geological blocks of Mongolia. The northern block consists of the Precambrian microcontinents and the Cambrian magmatic arc with the Lower Paleozoic oceanic and volcanic arc complexes. Variegated Lower to Upper Paleozoic sedimentary and volcanosedimentary units are exposed in the south. The adjoining units (the Lake Zone in the north and the Gobi-Altai Zone in the south) of these superterrane are imbricated in a complicated tectonic melange just along Main Mongolian Lineament. The valley of the Tsengel River (Fig. 1) intersects E–W oriented belts of Lower Paleozoic sequences belonging to the Gobi-Altai

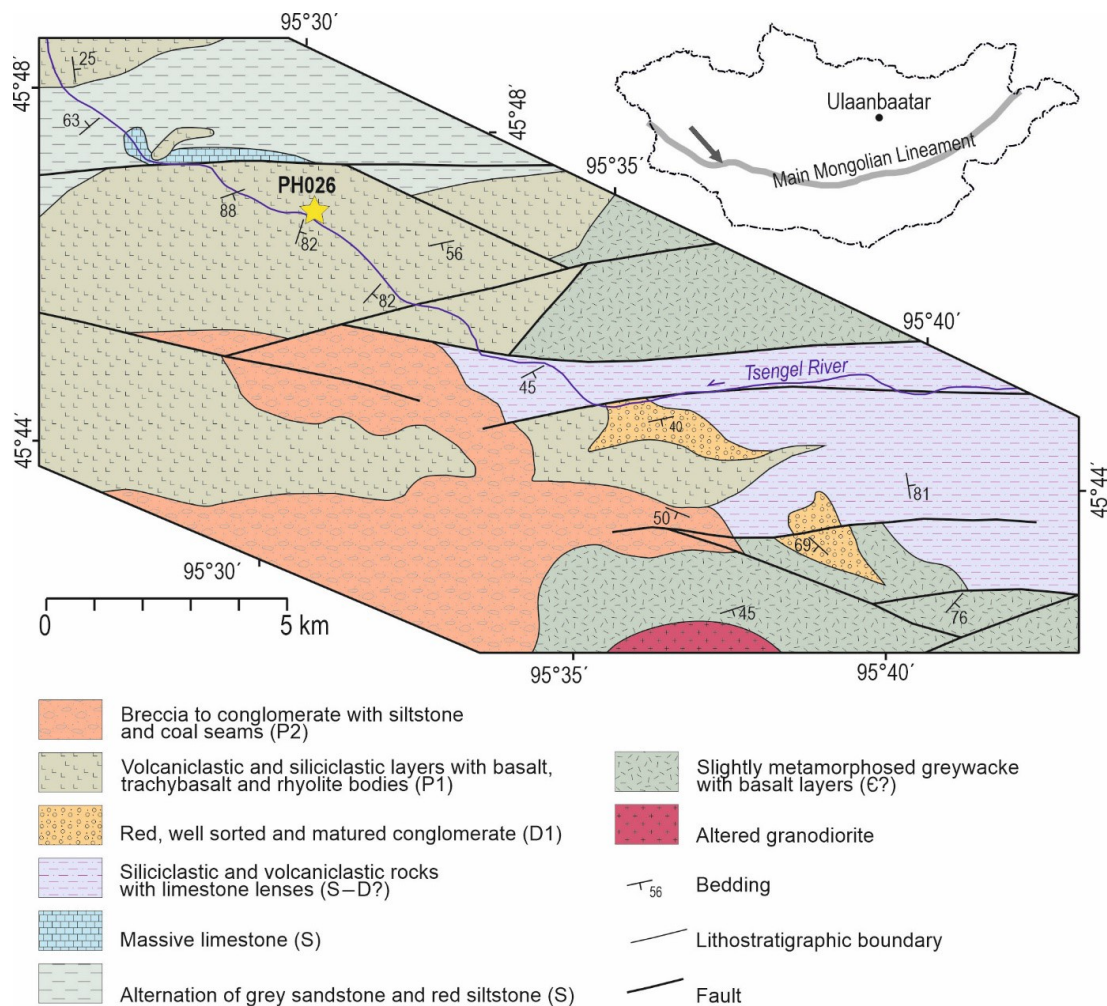


Fig. 1. Geological situation along the Tsengel River valley area in the Mongolian Altai. Modified from Togtokh et al. (1995).

Terrane in the sense of Badarch et al. (2002). These rocks are covered by Upper Permian continental sediments with coal seams. Newly described Lower Permian rocks were detached from to sequence depicted on the geological map 1: 200,000 as the Cambrian Durvuljiniuul Formation (Togtokh et al., 1995). They lie south of the E–W oriented significant fault, along which the layers of Silurian limestones are exposed. In the northern part of the Permian sequence, basic amygdaloid lavas predominate over volcanoclastic rocks and grey siltstones and sandstones. Varicolored siltstones with layers of coarse-grained sandstones, basalts and andesites dominate in the southern part. The bedding orientation is variable in the north and subvertical with predominant SW–NE strike in the south. The studied sample PH026 (WGS84 95.504677 E; 45.779629 N, Fig. 2A) was sampled from a massive medium-grained block of dark green lava (Fig. 2B) in agglomerate at the boundary of both subunits.

METHODOLOGY

Approximately 10 kg of rock was taken in the field at the reference point PH026 for geochemistry and heavy mineral separation.

The contents of the main and trace elements in the sample were determined in the ACTLabs laboratories by the ICP-MS method, the dissolution of the sample for the ICP-MS determination was performed in LiBO_2 / $\text{Li}_2\text{B}_4\text{O}_7$ (REE and high melting point metals) and aqua regia (precious metals). Whole rock analyses were processed using the GCDkit program (Janoušek et al., 2006).

The zircons were separated using conventional techniques (crushing, grinding, sieving, Wilfley gravity separation table, magnetic separation and separation in heavy liquids) at the Central Geological Laboratory in Ulaanbaatar. Subsequently, the individual zircons were manually selected from the zircon concentrate using a microscope, embedded in epoxy resin and polished. The internal structure and zoning of the selected zircon grains were studied by the cathodoluminescence (CL) method using a scanning electron microscope in laboratories of the Czech Geological Survey in Prague.

Analyses of mineral chemistry were performed

at a joint laboratory of the Faculty of Science of Masaryk University and the Czech Geological Survey in Brno on a Cameca SX-100 instrument using an accelerating voltage of 15 kV.

Zircons were dated by U-Pb using an Analyte Excite 193 nm excimer laser ablation system (LA, Proton Machines) equipped with a two-volume HelEx ablation cell in tandem with an Agilent 7900x ICPMS MSCP-MS (Agilent Technologies Inc., Santa Clara, USA) in laboratories of the Czech Geological Survey in Prague. The ablation took place in a He atmosphere (0.8 l. min^{-1}), the laser frequency was 5 Hz, the laser fluence was 7.59 J. cm^{-2} and the laser beam diameter was $25 \mu\text{m}$. Each measurement consisted of 20 s integration of the entrainment background signal and another 40 s integration of the sample ablation signal for masses 202, 204, 206, 207, 208, 232 and 238 using a SEM detector with one point per mass peak and mass integration time 10, 10, 15, 30, 20, 10 and 15 ms (total cycle time 0.134 s). To monitor the stability of the instrument and ensure the reliability of the measured results, zirconium standards (91500, Plešovice and GJ-1) were measured after every twenty samples. Instrumental drift throughout the measurement was monitored by repeated analyses of reference zircon 91500 (Wiedenbeck et al., 1995). The processing of the measured data was performed using Iolite software as is described in Paton et al. (2010), including background correction, followed by laser-induced elemental fractionation (LIEF) correction based on comparison with behaviour of reference zircon 91500 (1065 Ma, Wiedenbeck et al., 1995) whose concordant age $1062.9 \pm 2.8 \text{ Ma}$ measured during this study corresponds to the reference value. No correction was made for normal Pb. During this study, reference samples of Plešovice zircon (337 Ma, Sláma et al., 2008) and GJ-1 ($\sim 609 \text{ Ma}$, Jackson et al., 2004) were periodically analysed, which gave a concordant age of $337.8 \pm 1.7 \text{ Ma}$ and $609.3 \pm 2.3 \text{ Ma}$ (2σ), what corresponds to the reference values within the analytical error. Concordance diagrams and calculation of relevant U-Pb ages were processed by ISOPLOT / Ex version 3.0 (Ludwig, 2003).

RESULTS

Petrographical and geochemical characteristics

Sample PH026 is a medium-grained basaltic rock with an amygdaloidal structure and observable fluidal textures (Fig. 2C). The rock consists of altered glassy groundmass and pyroxene phenocrysts in, locally rimmed by amphibole and epidote grains. Amygdales are filled by chlorite and rarely by calcite. Chlorite, tiny epidote grains, Fe-oxides and titanite can be identified in the mass of devitrified glass (Fig. 2 C, D). Pyroxene is mostly hypautomorphic up to 6 mm in size, automorphic crystals are less common. The individual zones are relatively

"massive", having a diameter of 0.1 to 0.7 mm, the number of zones in individual grains ranges from 5 to 8. The pyroxene can be defined as diopside with a proportion of esseneite and a negligible admixture of alkaline pyroxenes. Well observable optical zoning reflects chemical composition with alternation of zones corresponding to 93.5–94.2 wt. % of diopside and zones in which the diopside content increases to 96.5–97 wt. %. The pyroxenes are sometimes replaced along the margins by a thin (10–15 μm) magnesiohornblende rim (Fig. 2D). In individual zones, it is possible to correlate the increase of Si, Mg and Cr with the decrease of Fe, Ti and Al contents and vice versa.

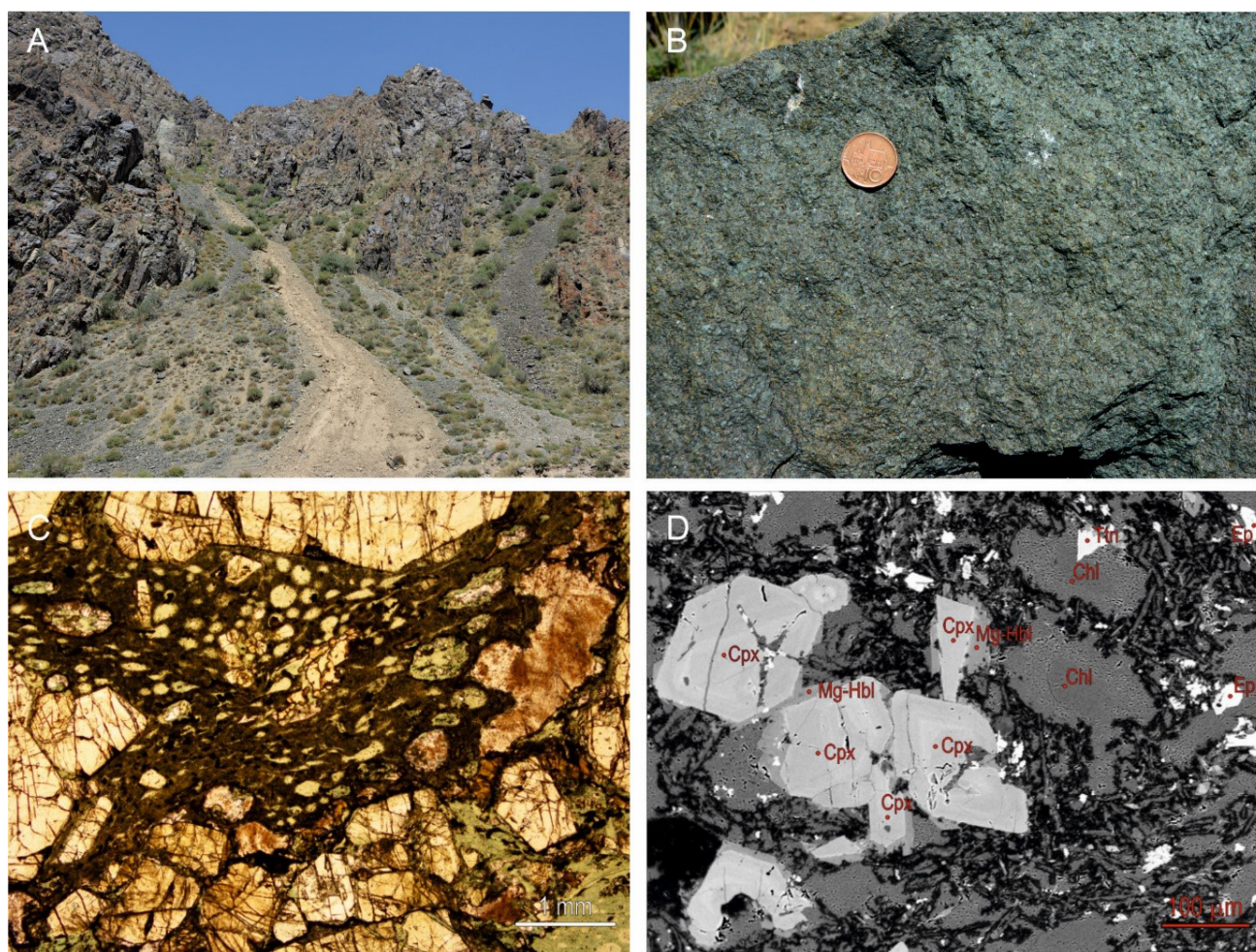


Fig. 2. A – Steeply oriented layers of tuffitic siltstones and sandstones with lenses of basaltic agglomerate (view towards east); B – Detail of sampled basalt fragment; C – Photomicrographs of the fluidal structures with altered glassy shards, flattened amygdales and auto - to hypautomorphic pyroxene phenocrysts are observable (plane-polarized light); D – The back-scattered electron (BSE) image illustrating pyroxene zoning and overgrowing of some pyroxene grains by amphibolite. The rock is further formed by chlorite, epidote, accessory titanite is also apparent.

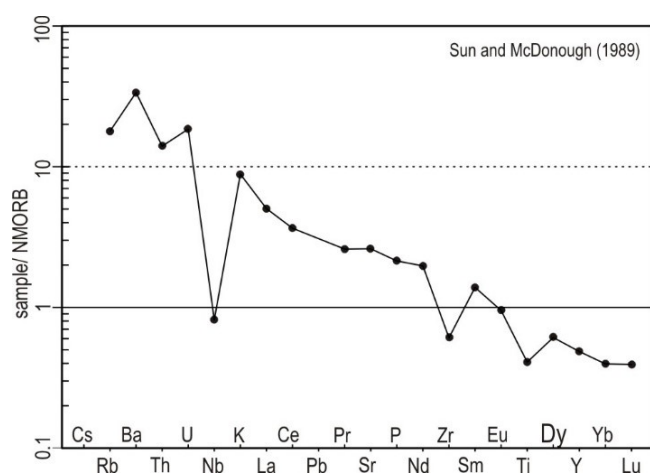


Fig. 3. Trace elements pattern of PH026 sample in spider plot, normalisation to NMORB (Sun and McDonough 1989).

Nevertheless, it should be noted that the chemical changes are negligible and pyroxene grains are quite uniform. The chlorite dispersed in the devitrified glass forms irregular flakes up to 100 μm in size of clinoclone composition with $X_{\text{Fe}} = 0.48$. The last observable mineral is the epidote, represented by cracked irregular grains about 100–150 μm in size, characterized by high relief and varicolored interference, chemically relatively inhomogeneous, with pistacite component contents of 32–55 mol%.

The chemical composition of the sample corresponds to basalt according the TAS classification (Le Bas 1986), as well as in the classification based on the contents of trace elements (Pearce 1996). Studied rock is thus a basalt with SiO_2 content 49.57 wt.%, with relatively high contents of FeOt (9.16 wt.%) and CaO (11.76 wt.%). The high mg # (71.6) corresponds to the position in the komatiitic basalt field in the Jensen (1976) classification. The normalized REE trend (Boynnton 1984) is weakly fractionated ($\text{La}_N/\text{Yb}_N = 7.02$) with a negligible negative Eu anomaly ($\text{Eu}/\text{Eu}^* = 0.85$). Compared to NMORB (Sun and McDonough 1989), the sample is enriched in LILE, Pb and Sr, shows significant negative anomaly in Nb and Ta, and less significant negative anomaly in Zr and Ti contents (Fig. 3). The contents of trace elements in geotectonic discrimination diagrams (e.g. Wood 1980; Agrawal et al. 2008; Pearce et al. 1984) correspond to a volcanic arc.

U-Pb LA ICP-MS zircon dating

Zircon grains are generally automorphic, transparent with a size from 50 \times 120 to 80 \times 300 μm . The crystals are shortly prismatic with an aspect ratio of 1:2 or 1:3 (with the exception of the long prismatic grain with an aspect ratio of 1:5, Fig. 4A) with rounded fuzzy edges and short pyramids, pastel luster and light honey-like color. However, fragments of broken originally automorphic to hypautomorphic grains prevail. The magmatic oscillatory zoning of most of the zircon grains is clear in the CL, in some cases it is possible to observe the replacement of the oscillatory zoning by sector zoning. Sometimes also different degrees of recrystallization, or even resorption of the grain is present (Fig. 5). Three of the studied grains (No. 28, 30 and 31; Fig 6, Table 1) show only minimal luminescence in the CL image, what together with their anomalous young age, indicates higher relative U contents.

Four age groups can be distinguished in the whole set of 44 measured spots on zircons from sample PH026:

- 1) The oldest (Upper Devonian) ages with a weighted average of 376 ± 4.7 Ma (Fig. 7, Table 1) were found in two grains: In one of the inner zones, in a sample of an atypical, long prismatic 370 μm long zircon grain (No. 45; spot 1; Fig. 4A) with a clear oscillatory zoning and in the marginal zone of a well crystallized automorphic short prismatic grain (No. 19), with sector zoning replacing original oscillatory zoning with the small number of relatively massive (approx. 10 μm) individual zones. Marginal zones in this grain show signs of later probably magmatic dissolution (Fig. 4B).
- 2) The second group yielding the Lower Carboniferous age of 351.9 ± 3.5 Ma (Fig. 7) was determined in the marginal zone of the automorphic long prismatic long grain mentioned above (No. 45; spot 2; Fig. 4A). Furthermore, these ages were found in three spots across short prismatic 360 μm long oscillatory zoned zircon (No. 15; spots 1, 2 and 3; Fig. 4C) with oval quartz inclusions and in the central part of a fragment of an automorphic short prismatic grain (No. 35; Fig. 4D) with detailed very fine oscillatory

zoning. All of these three grains (No. 45, 15, 35; Fig. 4A, C, D) morphologically differ from each other studied zircons. No. 45 grain differs in a long prismatic shape, the other in sizes, detailed zoning, darker luminescence and in grain No. 15 in a large number of quartz inclusions. Therefore, it can be assumed that these represent xenocrysts (long prismatic grain) and/or clastic zircons, that have contaminated ascending magma. The dominant ages – 34 of the total 44 measurements – form two groups: 304.4 ± 2.3 Ma and 288.6 ± 1.9 Ma (Fig. 7, Table 1).

3) Eleven measurements correspond to Upper

Carboniferous age of 304.4 ± 2.3 Ma. These ages were measured in: (a) the centres of fragments of originally automorphic short prismatic grains with well-developed oscillatory zoning (No. 7, 8; Fig. 5A, B); (b) the central part of originally automorphic oscillatory zoned grains with clear traces of dissolution, recrystallization and later growth (No. 69; Fig. 5C) and (c) incremental zones of partly dissolved grains (No. 33; Fig. 5D).
4) The other 23 data document weighted average age of 288.6 ± 1.9 Ma (Lower Permian) measured in the central as well as in the incremental zones of short prismatic grains,

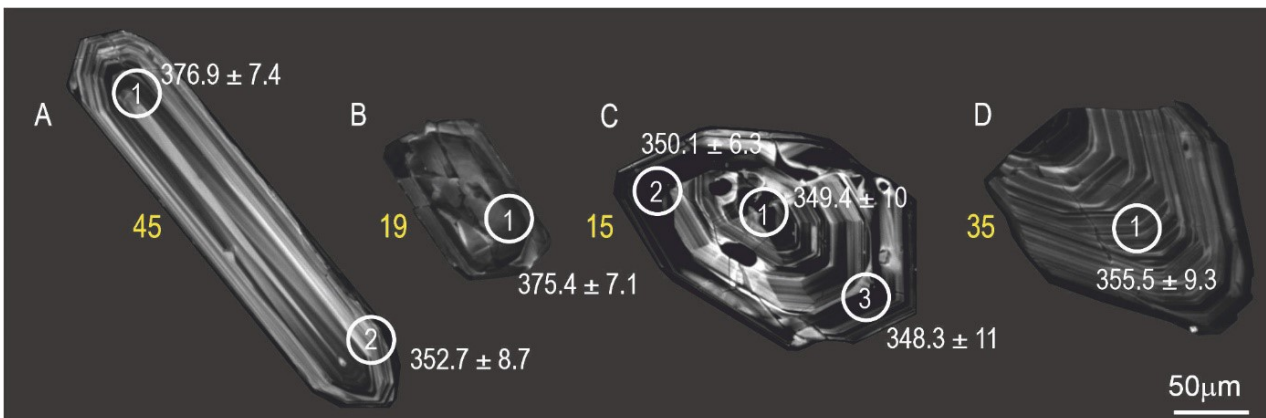


Fig. 4. Upper Devonian and Lower Carboniferous zircon generation separated from PH026 and dated using laser ablation in CL image. Yellow numbers correspond to grain number in Table 1.

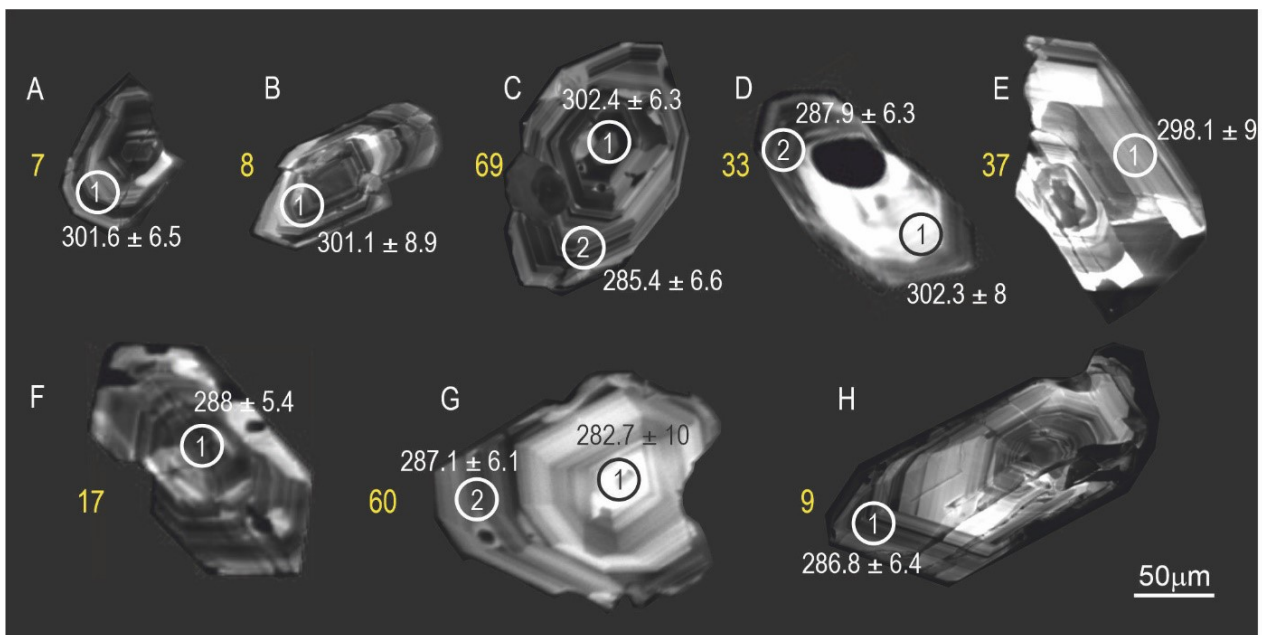


Fig. 5. Example of zircon grains providing the Upper Carboniferous to Lower Permian magmatic ages of the rock in the CL image.

usually with rounded edges of pyramids. These are usually oscillatory zoned; sector zoning is less frequent but not exceptional (grains No. 37, 17, 60, 9; Fig. 5E, F, G, H).

- 5) The youngest Upper Triassic age 218 ± 3.4 Ma (Fig. 7, Table 1) was detected in three of studied grains (Fig. 6). First grain (No. 31) is a hypautomorphic, very slightly luminescent short prismatic $125 \mu\text{m}$ long grain with indistinct simple zoning formed by the core and two darker incremental zones about $8 \mu\text{m}$ thick, separated by a lighter thin zone (Fig. 6A). The second grain (No. 30) is non-luminescent short prismatic automorphic $150 \mu\text{m}$ long grain with a noticeable indistinct original oscillatory zoning replaced by a more distinct sector zoning (Fig. 6B). The last one (No. 28) is a nearly non-luminescent short prismatic grain $90 \mu\text{m}$ long with an indistinct simple zoning, formed by a dark core and a slightly lighter $12 \mu\text{m}$ thick marginal zone (Fig. 6C). The indistinct luminescence of zircons suggests the lead loss resulting in geologically improbable Triassic age.

SUMMARY AND DISCUSSION

The new occurrence of Permian volcanic and volcanoclastic rocks was found in the valley of the Tsengel River (western Gobi-Altai Terrane of Badarch et al., 2002) inside the area formerly considered to be Lower Paleozoic (Togtokh et al., 1995). The studied sample forms a massive

part of fluidal agglomerate lava and it is classified as pyroxene basalt composed of glassy matrix with pyroxene phenocrysts. The chemical composition of this high-Mg basalt does not correspond to the alkaline character of Permian intraplate volcanism described further to the east in the Khar Argalantyn area by Buriánek et al. (2012) or on the NE slopes of the Khantaishir ridge by Kozakov et al. (2015).

Dominating concordia cluster with two age peaks corresponding to 288 Ma resp. 304 Ma is associated with two consecutive magmatic events in relatively near time succession of uppermost Carboniferous – Lower Permian age. Inherited zircons of two groups with an age of ~ 376 resp. 352 Ma probably reflect Devonian to Carboniferous magmatic events in wider surroundings. Ages of c. 380–370 Ma are known from granitic rocks of the metamorphic unit Tseel lying south of the studied area (Burenjargal et al. 2014, 2016; Hanžl et al. 2016; Cai et al. 2015). Ages of c. 350 Ma are known from the granite massifs of the Mongolian Altai further west (Cai et al. 2015) or from the Chandman Massif in the east (Hrdličková et al., 2008; Lehmann et al., 2017). The basalt agglomerate represents the final stage of arc magmatism, which was reported over the subduction zone retreating towards the south in the Trans-Altai Gobi further to the south (Nguyen et al. 2018) or the extension phase immediately following the subduction plate break-off, as described by Buriánek et al. (2016)

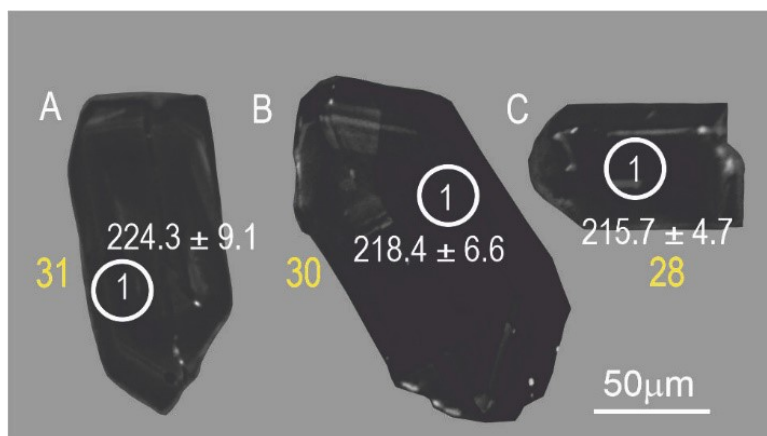


Fig. 6. The example of insignificantly luminescent zircon grains yielding the Triassic age.

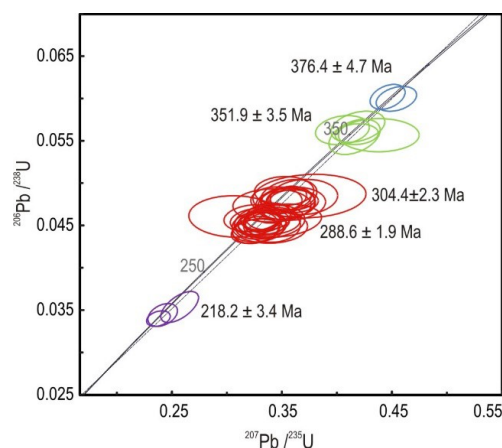


Fig. 7. U-Pb concordia diagram for zircons from PH026 sample. All data are plotted with 2σ uncertainties.

Table 1. Laser ablation ICP-MS U-Pb zircon data for PH026 sample.

Spot name	Corrected isotopic ratios							Apparent ages (Ma)					
	207Pb	±2SE	206Pb	±2SE	207Pb	±2SE	Rho	207Pb	±2SE	206Pb	±2SE	207Pb	±2SE
	235U	(abs.)	238U	(abs.)	206Pb	(abs.)	6/8 vs. 7/5	235U	(Ma)	238U	(Ma)	206Pb	(Ma)
<i>Sample CTRZ1 (n=57)</i>													
18004_PH026_1	0.934	0.051	0.0515	0.0014	0.131	0.0059	0.40646	660	26	323.8	8.8	2068	93
18004_PH026_2	0.494	0.028	0.0498	0.0013	0.0724	0.0042	0.026114	403	19	313.3	7.9	880	120
18004_PH026_4	0.794	0.031	0.04975	0.0011	0.115	0.004	0.16155	591	17	312.9	6.7	1862	68
18004_PH026_5	0.335	0.015	0.04518	0.0011	0.0544	0.0024	0.1459	293	12	284.8	7	367	99
18004_PH026_7	0.361	0.018	0.04792	0.0011	0.055	0.0028	0.012262	310	14	301.6	6.5	320	100
18004_PH026_8	0.356	0.02	0.0478	0.0014	0.0547	0.0032	-0.037878	307	15	301.1	8.9	340	120
18004_PH026_9	0.331	0.015	0.04551	0.001	0.0532	0.0025	-0.058817	289	11	286.8	6.4	289	97
18004_PH026_10	0.477	0.029	0.0464	0.0014	0.0746	0.0047	0.10075	394	20	292.3	8.8	990	120
18004_PH026_14	0.354	0.015	0.0482	0.0012	0.0531	0.002	0.28618	306	11	303.2	7.5	287	80
18004_PH026_15_1	0.438	0.03	0.0557	0.0016	0.0573	0.004	0.0095573	367	21	349.4	10	450	150
18004_PH026_15_2	0.418	0.016	0.05582	0.001	0.0543	0.0016	0.10214	354.4	11	350.1	6.3	368	67
18004_PH026_15_3	0.416	0.019	0.0555	0.0017	0.0542	0.0021	0.38834	353	13	348.3	11	373	90
18004_PH026_17	0.332	0.013	0.04559	0.00088	0.0534	0.0019	0.22849	291.8	10	287.3	5.4	294	76
18004_PH026_18	0.307	0.034	0.0461	0.002	0.0499	0.0059	-0.031982	258	26	290	12	-10	200
18004_PH026_19	0.454	0.015	0.05999	0.0012	0.0551	0.0014	0.32152	378.3	10	375.4	7.1	379	57
18004_PH026_20	1.28	0.14	0.0674	0.0055	0.144	0.02	0.0696	823	62	420	33	2140	230
18004_PH026_22_1	0.33	0.022	0.0455	0.0013	0.0536	0.0034	0.078417	285	16	286.7	7.9	250	130
18004_PH026_22_2	0.352	0.022	0.0491	0.0014	0.053	0.0034	0.041288	301	16	309.6	8.9	210	130
18004_PH026_25	0.428	0.032	0.0468	0.0015	0.0676	0.0053	0.088398	354	22	294.7	9	660	160
18004_PH026_27_1	0.341	0.014	0.04649	0.00096	0.0536	0.0022	0.074222	296.1	11	292.9	5.9	303	86
18004_PH026_27_2	0.356	0.021	0.0485	0.0016	0.0539	0.0031	0.25963	306	15	305.3	9.5	290	120
18004_PH026_26	0.375	0.042	0.0485	0.0021	0.0577	0.0066	0.10474	313	31	305	13	300	230
18004_PH026_28	0.2377	0.0088	0.03403	0.00075	0.0508	0.0015	0.3037	216	7.2	215.7	4.7	219	68
18004_PH026_29	0.348	0.031	0.0456	0.0016	0.0564	0.0048	0.20894	301	23	287.5	10	390	180
18004_PH026_30	0.2416	0.011	0.03446	0.0011	0.0512	0.0021	0.36899	219.4	8.8	218.4	6.6	230	91
18004_PH026_31	0.257	0.014	0.0354	0.0015	0.0524	0.0024	0.60006	232	12	224.3	9.1	290	100
18004_PH026_32	0.326	0.018	0.0444	0.0012	0.0539	0.0026	0.312	285	13	279.9	7.2	320	110
18004_PH026_33_1	0.345	0.019	0.048	0.0013	0.0535	0.0033	0.0062397	299	15	302.3	8	250	120
18004_PH026_33_2	0.331	0.015	0.04569	0.001	0.0526	0.0023	0.10991	288	11	287.9	6.3	255	92
18004_PH026_35	0.419	0.02	0.0567	0.0015	0.0542	0.0023	0.32131	354	14	355.5	9.3	343	94
18004_PH026_36	0.446	0.018	0.04207	0.001	0.0783	0.0032	0.19645	376	13	265.5	6.3	1092	78
18004_PH026_37	0.341	0.029	0.0474	0.0016	0.0527	0.0045	0.037231	290	22	298.1	9.7	170	170
18004_PH026_38	0.323	0.021	0.0459	0.0013	0.0513	0.0034	0.1646	283	17	289.4	8.1	190	130
18004_PH026_39	0.434	0.022	0.0469	0.0015	0.0674	0.0033	0.24221	364	15	295.5	9.1	780	100
18004_PH026_41	0.328	0.019	0.04444	0.0011	0.0526	0.0029	0.14307	286	15	280.2	6.8	270	110
18004_PH026_42	0.419	0.028	0.0467	0.0017	0.0653	0.0047	0.11226	352	20	294	11	680	150
18004_PH026_45_1	0.446	0.013	0.06023	0.0012	0.0537	0.0013	0.36722	373.1	9.4	376.9	7.4	340	53
18004_PH026_45_2	0.405	0.02	0.0563	0.0014	0.0516	0.0024	0.2019	343	14	352.7	8.7	232	98
18004_PH026_47	0.341	0.021	0.045	0.0016	0.055	0.0034	0.043077	297	16	283.4	9.6	370	140
18004_PH026_48	0.326	0.017	0.0445	0.0013	0.0536	0.0027	0.20875	284	13	280.6	8.1	280	110
18004_PH026_49	0.332	0.018	0.0451	0.0012	0.0531	0.0031	0.023848	290	14	284.5	7.4	280	120
18004_PH026_52	0.573	0.046	0.0478	0.0019	0.0915	0.0079	0.10767	445	30	300	11	1080	180
18004_PH026_53	0.341	0.021	0.0456	0.0013	0.0541	0.0033	0.047723	293	16	287.5	7.8	290	130
18004_PH026_54	0.359	0.025	0.0476	0.0016	0.0556	0.0041	0.11561	308	19	299.8	9.8	320	150
18004_PH026_57	0.338	0.017	0.0461	0.0013	0.053	0.0027	0.10411	294	13	290.4	7.9	270	110
18004_PH026_60_1	0.339	0.028	0.0449	0.0016	0.055	0.0045	0.024856	294	22	282.7	10	290	170
18004_PH026_60_2	0.332	0.014	0.04555	0.001	0.0528	0.0021	0.2251	289.7	11	287.1	6.1	271	86
18004_PH026_61	0.37	0.025	0.0484	0.0017	0.0568	0.0041	0.080309	313	19	304.4	10	330	140
18004_PH026_64	1.496	0.071	0.0553	0.0018	0.1952	0.0086	0.36775	925	31	347	11	2752	78
18004_PH026_66	0.357	0.016	0.04824	0.0011	0.0536	0.0023	0.176	309	12	303.6	6.8	294	89
18004_PH026_67	0.533	0.018	0.0583	0.0011	0.0655	0.002	0.13357	433	12	365.2	6.7	779	61
18004_PH026_68	1.301	0.09	0.054	0.0016	0.173	0.011	0.39548	819	41	339	10	2470	110
18004_PH026_69_1	0.358	0.018	0.04804	0.001	0.0541	0.0026	0.065392	308	13	302.4	6.3	290	100
18004_PH026_69_2	0.326	0.016	0.04529	0.0011	0.0516	0.0023	0.13474	285	12	285.4	6.6	230	96
18004_PH026_70	0.353	0.022	0.0476	0.0015	0.0544	0.0033	0.14475	305	16	299.5	9.2	350	130
18004_PH026_71	0.331	0.019	0.045	0.0013	0.054	0.0031	0.15191	290	15	283.9	8.2	290	120
18004_PH026_74	0.339	0.026	0.0455	0.0016	0.0539	0.004	0.14318	295	19	286.6	10	320	160

on the example of the Permian to Carboniferous Sagsai pluton situated about 75 km SE from the studied locality.

ACKNOWLEDGEMENTS

The sample was taken and processed within the GACR project No. 19-27682X. "Principal mechanisms of peripheral continental growth during supercontinent cycle", carried by K. Schulmann. The analytical work was co-financed by the internal project 310240 of the Czech Geological Survey "Genesis of postorogenic granites of the Aaj Bogd massif in the Transaltai zone in southwestern Mongolia". The authors thank to J. Haifler and P. Gadas for their cooperation on mineral analysis. Special thanks to K. Breiter and M. Svojtka for their advice and comments. Last but not least we express gratitude to the editor and reviewers of the manuscript.

REFERENCES

- Agrawal, S., Guevara, M., Verma, S.P. 2008. Tectonic discrimination of basic and ultrabasic volcanic rocks through log-transformed ratios of immobile trace elements: *International Geology Review* v. 50, p. 1057-1079. <https://doi.org/10.2747/0020-6814.50.12.1057>
- Badarch, G., Cunningham, W. D., Windley B. F. 2002. A new terrane subdivision for Mongolia: Implications for the Phanerozoic crustal growth of central Asia: *Journal of Asian Earth Sciences* 21(1), p. 87-110. [https://doi.org/10.1016/S1367-9120\(02\)00017-2](https://doi.org/10.1016/S1367-9120(02)00017-2)
- Boynton W. V. 1984. Cosmochemistry of the rare earth elements: meteorite studies. In: Henderson P. ed.: *Rare Earth Element Geochemistry*, p. 63-114., Elsevier, Amsterdam. <https://doi.org/10.1016/B978-0-444-42148-7.50008-3>
- Burenjargal, U., Okamoto, A., Kuwatani, T., Sakata, S., Hirata, T., Tsuchiya, N. 2014. Thermal evolution of the Tseel Terrane, SW Mongolia and its relation to granitoid intrusions in the Central Asian Orogenic Belt: *Journal of Metamorphic Geology* v. 32, p. 765-790. <https://doi.org/10.1111/jmg.12090>
- Burenjargal, U., Okamoto, A., Tsuchiya, N., Uno, M., Horie, K., Hokada, T. 2016. Contrasting geochemical signatures of Devonian and Permian granitoids from the Tseel Terrane, SW Mongolia: *Journal of Geosciences* v. 61, 51-66. <https://doi.org/10.3190/jgeosci.210>
- Buriánek, D., Hanžl, P., Budil, P., Gerdes, A. 2012. Evolution of the Early Permian volcanic-plutonic complex in the western part of the Permian Gobi-Altay Rift (Khar Argalant Mts., SW Mongolia): *Journal of Geosciences* v 57 (2), 105-126. <https://doi.org/10.3190/jgeosci.116>
- Buriánek, D., Janoušek, V., Hanžl, P., Jiang, Y., Schulmann, K., Lexa, O., Altanbaatar, B. 2016. Petrogenesis of the Late Carboniferous Sagsai Pluton in the SE Mongolian Altai: *Journal of Geosciences* v. 61, p. 67-92. <https://doi.org/10.3190/jgeosci.207>
- Cai, K., Sun, M., Jahn, B. M., Xiao, W. J., Yuan, C., Long, X., Chen, H., Tumurkhuu, D. 2015. A synthesis of zircon U-Pb ages and Hf isotopic compositions of granitoids from southwest Mongolia: implications for crustal nature and tectonic evolution of the Altai Superterrane: *Lithos* v. 232, p. 131-142. <https://doi.org/10.1016/j.lithos.2015.06.014>
- Hanžl, P., Bat-Ulzii, D., Rejchrt, M., Košler, J., Bolormaa, K., Hrdličková, K. 2008. Geology and geochemistry of the Palaeozoic plutonic bodies of the Trans-Altay Gobi, SW Mongolia: Implications for magmatic processes in an accreted volcanic-arc system. *Journal of Geosciences* v. 53 (2), p. 201-234. <https://doi.org/10.3190/jgeosci.028>
- Hanžl, P., Schulmann, K., Janoušek, V., Lexa, O., Hrdličková, K., Jiang, Y., Buriánek, D., Altanbaatar, B., Ganchuluun, T., Erban, V. 2016. Making continental crust: origin of Devonian orthogneisses from SE Mongolian Altai: *Journal of Geosciences* v. 61, p. 1-10. <https://doi.org/10.3190/jgeosci.206>
- Hanžl, P., Guy, A., Battushig, A., Lexa, O., Schulmann, K., Kunceová, E., Hrdličková, K., Janoušek, V., Buriánek, D., Krejčí, Z., Jiang, Y., Otgonbator, D. 2020. Geology of the Gobi and Mongol Altai junction enhanced by gravity analysis: a key for understanding of the Mongolian Altaides. *Journal of Maps* v. 16 (2), p. 98-107. <https://doi.org/10.1080/17445647.2019.1700835>
- Hrdličková, K., Bolormaa, K., Buriánek, D., Hanžl, P., Gerdes, A., Janoušek, V. 2008.

- Petrology and age of metamorphosed rocks in tectonic slices inside the Palaeozoic sediments of the eastern Mongolian Altay, SW Mongolia: *Journal of Geosciences* v. 53, p. 139-165. <https://doi.org/10.3190/jgeosci.027>
- Jackson, S.E., Pearson, N.J., Griffin, W.L., Belousova, E.A., 2004. The application of laser ablation-inductively coupled plasma-mass spectrometry to in situ U-Pb zircon geochronology: *Chemical Geology* v. 211, p. 47-69. <https://doi.org/10.1016/j.chemgeo.2004.06.017>
- Janoušek, V., Farrow, C. M., Erban, V. 2006. Interpretation of whole-rock geochemical data in igneous geochemistry: introducing Geochemical Data Toolkit (GCDkit): *Journal of Petrology* v. 47, p. 1255-1259. <https://doi.org/10.1093/petrology/egl013>
- Janoušek, V., Jiang, Y., Buriánek, D., Schulmann, K., Hanžl, P., Soejono, I., Kröner, A., Altanbaatar, B., Erban, V., Lexa, O., Ganchuluun, T., Košler J. 2018. Cambrian-Ordovician magmatism of the Ikh-Mongol Arc System exemplified by the Khantaishir Magmatic Complex (Lake Zone, south-central Mongolia): *Gondwana Research* v. 54, p. 122-149. <https://doi.org/10.1016/j.gr.2017.10.003>
- Jensen, L. S., 1976. A new cation plot for classifying sub-alkaline volcanic rocks Ontario Division Mines Miscellaneous Paper No. 66 p. 1-22.
- Kozakov, I. K., Kirnozova, T. I., Kovach, V. P., Terent'eva, L. B., Tolmacheva, E. V., Fugzan, M. M., Erdenezhargal, Ch. 2015. Late Riphean age of the crystalline basement of the carbonate cover of the Dzabkhan microcontinent: *Stratigraphy and Geological Correlation* v. 23, p. 237-245. <https://doi.org/10.1134/S0869593815030041>
- Kozlovsky, A.M., Yarmolyuk, V.V., Sal'nikova, E.B., Travin, A.V., Kotov, A.B., Plotkina, J.V., Kudryashova, E.A., Savatenkov, V.M. 2015. Late Paleozoic anorogenic magmatism of the Gobi Altai (SW Mongolia): tectonic position, geochronology and correlation with igneous activity of the Central Asian Orogenic Belt: *Journal of Asian Earth Sciences* v. 113, p. 524-541. <https://doi.org/10.1016/j.jseaes.2015.01.013>
- Le Bas M.J., Le Maitre R.W., Streckeisen A., Zanettin B. 1986. A Chemical Classification of Volcanic Rocks Based on the Total Alkali-Silica Diagram. *Journal of Petrology* v. 27, p.745-750. <https://doi.org/10.1093/petrology/27.3.745>
- Lehmann, J., Schulmann, K., Lexa, O., Závada, P., Štípská, P., Hasalová, P., Belyanin, G., Corsini, M. 2017. Detachment folding of partially molten crust in accretionary orogens: A new magma-enhanced vertical mass and heat transfer mechanism: *Lithosphere* v. 9 (6). p. 889-909. <https://doi.org/10.2475/07.2010.02>
- Ludwig, K.R. 2003. Isoplot 3.00: A geochronological toolkit for Microsoft Excel: Berkeley Geochronology Center Special Publication.
- Mossakovsky, A.A., Ruzhentsev, S.V., Samygin, S.G., Kheraskova, T. N. 1993. The Central Asian fold belt: geodynamic evolution and formation history: *Geotectonics* v. 26, p. 455-473.
- Nguyen, H., Hanžl, P., Janoušek, V., Schulmann, K., Ulrich, M., Jiang, Y., Lexa O., Altanbaatar, B., Deiller, P. 2018. Geochemistry and geochronology of Mississippian volcanic rocks from SW Mongolia: Implications for terrane subdivision and magmatic arc activity in the Trans-Altai Zone: *Journal of Asian Earth Sciences* v. 164, p. 322-343. <https://doi.org/10.1016/j.jseaes.2018.06.029>
- Paton, C., Woodhead, J.D., Hellstrom, J.C., Hergt, J.M., Greig A., Maas, R. 2010. Improved laser ablation U-Pb zircon geochronology through robust downhole fractionation correction: *Geochemistry, Geophysics, Geosystems*, v. 11(3), p. 1-36. <https://doi.org/10.1029/2009GC002618>
- Pearce, J. 1996. Sources and setting granitic rocks: *Episodes* v. 19 (4), p. 120-125. <https://doi.org/10.18814/epiiugs/1996/v19i4/005>
- Pearce, J. A., Harris, N. W., Tindle, A. G. 1984. Trace element discrimination diagrams for the tectonic interpretation of granitic rocks: *Journal of Petrology* v. 25, p. 956-983. <https://doi.org/10.1093/petrology/25.4.956>
- Sibley, D. F., Vogel, T. A., Walker, B. M., Byerly, G. 1976. The origin of oscillatory

- zoning in plagioclase: a diffusion and growth controlled model: *American Journal of Science* v. 276, p. 275-284.
<https://doi.org/10.2475/ajs.276.3.275>
- Sláma, J., Košler, J., Condon, D.J., Crowley, J.L., Gerdes, A., Hanchar, J.M., Horstwood, M.S.A., Morris, G.A., Nasdala, L., Norberg, N., Schaltegger, U., Schoene, B., Tubrett, M.N., Whitehouse, M.J. 2008. Plešovice zircon-A new natural reference material for U-Pb and Hf isotopic microanalysis. *Chemical Geology* v. 249, p. 1-35.
<https://doi.org/10.1016/j.chemgeo.2007.11.005>
- Soejono, I., Buriánek, D., Svojtka, M., Žáček, V., Čáp, P., Janoušek, V. 2016. Mid-Ordovician and Late Devonian magmatism in the Togtokhinshil Complex: new insight into the formation and accretionary evolution of the Lake Zone (western Mongolia): *Journal of Geosciences* v. 61 (1), p. 5-23.
<https://doi.org/10.3190/jgeosci.208>
- Sun, S. S., McDonough, W. F. 1989. Chemical and isotopic systematics of oceanic basalts: implications for mantle composition and processes. In: Saunders, A.D., Norry, M.J. (eds) *Magmatism in ocean basins*: Geological Society of London, v. 42. Special Publications, p. 313-345.
<https://doi.org/10.1144/GSL.SP.1989.042.01.19>
- Togtokh, D., Baatarkhuiag, A., Bayadalai, S., Usna-Ekh, C. 1995. Tonkhilyn I-Rangin 1988-1991 онд xiisen 1 : 200 000-ny masshatabtai geologiin bulegchilcen zuralalyn ur dungiin tajjlan. - MS MRPAM.
- Wiedenbeck, M., Allé, P., Corfu, F., Griffin, W.L., Meier, M., Oberli F., Von Quadt A., Roddick J.C., Spiegel W. 1995. Three natural zircon standards for U-Th-Pb, Lu-Hf, trace element and REE analyses: *Geostandards and Geoanalytical Research* v. 19 (1), p. 1-23.
<https://doi.org/10.1111/j.1751-908X.1995.tb00147.x>
- Windley, B. F., Alexeiev, D., Xiao, W., Kroner, A., Badarch, G. 2007. Tectonic models for the accretion of the Central Asian orogenic belt: *Journal of the Geological Society of London* v. 164(1), 31-47.
<https://doi.org/10.1144/0016-76492006-022>
- Wood, D. A. 1980. The application of a Th-Hf-Ta diagram to problems of tectonomagmatic classification and to establishing the nature of crustal contamination of basaltic lavas of the British Tertiary volcanic province: *Earth and Planetary Science Letters* v. 50, p. 11-30.
[https://doi.org/10.1016/0012-821X\(80\)90116-8](https://doi.org/10.1016/0012-821X(80)90116-8)